ACS Sustainable Chemistry & Engineering

pubs.acs.org/journal/ascecg

Letter

Visible-Light-Driven Chlorine-Atom-Mediated Efficient and Selective Cleavage of C−C Bond in Lignin Models

Pengju Li, Rong Liu, Zijian Zhao, Weijian Yang, Fushuang Niu, Limei Tian, and Ke Hu*

Cite This: *ACS Sustainable Chem. Eng.* 2024, 12, 10−17

Read Online

ACCESS | Metrics & More | Article Recommendations | Supporting Information

ABSTRACT: Lignin valorization to aromatic fine chemicals requires selective cleavage of a high-energy C−C bond under mild conditions. Herein, we report the efficient and selective C−C bond cleavage of lignin model substrates through a chlorine (Cl) atom as the hydrogen atom transfer agent generated by visible-light excitation of the metal-free photocatalyst perylene diimide. With the assistance of the Cl atom, the overall yield of C−C bond cleavage products in model substrate β−O−4 linkages reached 82.5% under visible-light excitation. This work makes use of metal-free photocatalysts and ubiquitous chloride as an alternative sustainable method for lignin depolymerization.

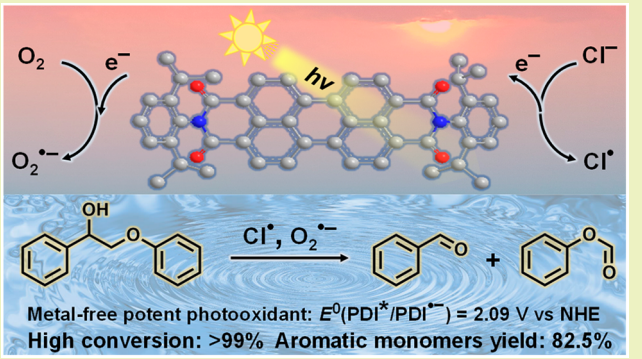

KEYWORDS: *Perylene Diimide Photocatalyst, Chloride Oxidation, HAT Agent, C−C Bond Cleavage, Biomass Valorization*

INTRODUCTION

Lignin is a natural and sustainable source of aromatic compounds that can be converted to renewable fuels and other high-value products. The depolymerization of lignin, however, is hindered by the difficulty of breaking C−C bonds that have high dissociation energy and low reactivity.[1−5] Photocatalysis offers a promising strategy for the solar-driven valorization of lignin. Prior studies have demonstrated the use of metal complexes[3,6] or semiconductors[7,8] to generate reactive species that can cleave C−C bonds, yet the selectivity and yield of this energy-demanding process are still unsatisfactory. A possible solution is to employ hydrogen atom transfer (HAT) agents[9−16] that can selectively activate reactive sites and enhance the C−C bond cleavage efficiency.

The chlorine (Cl) atom as a reactive intermediate as well as an HAT agent is widely used in the study of C(sp^3)−H bond activation.[17−24] It could be produced from the oxidation of cheap and readily available chloride salts. However, the production of Cl atoms by photoredox catalysis is generally based on noble metal photocatalysts such as ruthenium- or iridium-based inorganic coordination compounds because the single-electron reduction potential ($Cl^{\bullet/-}$) requires a strong photooxidant.[25,26] Furthermore, those photocatalysts mostly absorb only the blue part of the solar spectrum, making it fairly inefficient for solar energy utilization.

Herein, we report a visible-light-promoted Cl-atom-mediated efficient and selective cleavage of the lignin model C−C bond in a metal-free photocatalyst and additive-free manner under mild ambient conditions. Under visible-light excitation, the perylene diimide (PDI) excited state oxidatively cleaved the C−C bond in lignin β−O−4 linkages to form benzaldehyde and phenyl formate, and the C−C bond cleavage selectivity can be improved based on the HAT process mediated by Cl atom. In addition, we also found that the Cl atom can greatly improve the yield of β−1 linkages model cleavage products. We believe this study provides new insights into C−C bond cleavage induced by the Cl atom.

RESULTS AND DISCUSSION

The photocatalyst PDI was prepared according to the procedure reported in the literature.[27] The ground state UV−vis absorption spectrum of PDI in CH_3CN is shown in Figure 1a. Three characteristic absorption peaks are at 456, 487, and 523 nm. The fluorescence spectrum of PDI mirrors the absorption spectrum with peaks at 533, 573, and 620 nm. The free energy stored in the PDI excited state (E_{0-0}) can be estimated from the intersection of the absorption and fluorescence spectra and is found to be 2.35 eV. Cyclic voltammetry (CV) was carried out to measure the redox properties of the PDI (Figure 1b). Two reversible redox waves are observed upon PDI reduction. The potential of the PDI/$PDI^{\bullet-}$ redox couple was obtained from the first redox wave,

Received: July 18, 2023
Revised: December 7, 2023
Accepted: December 19, 2023
Published: December 27, 2023

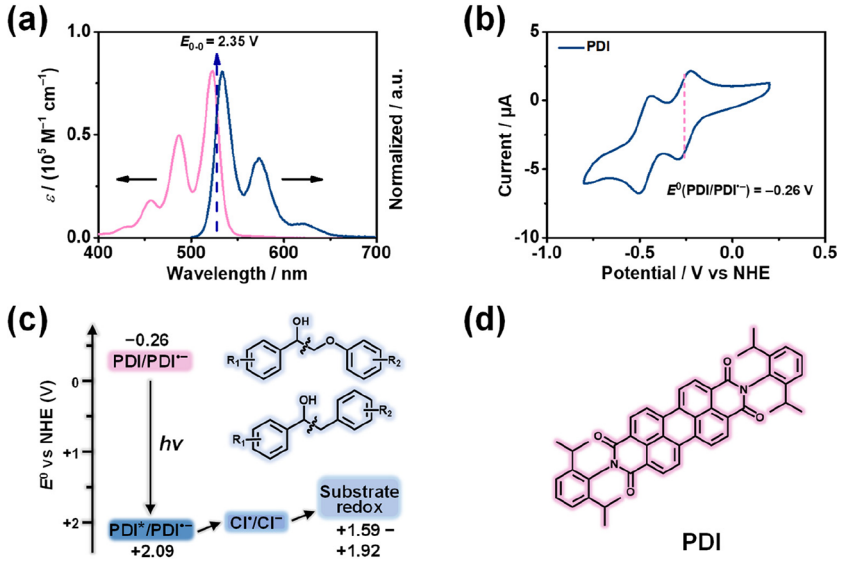

Figure 1. (a) Ground state UV−vis absorption and fluorescence spectra (λ_{ex} = 480 nm) of PDI in CH_3CN solution under ambient air. (b) Cyclic voltammogram of PDI in 100 mM $TBAClO_4$ CH_3CN solution under argon (scan rate: 50 mV s^{-1}). (c) Energetic diagram of PDI for Cl-atom-mediated C−C bond cleavage of the lignin model upon visible-light excitation. (d) Molecular structure of PDI used in this study.

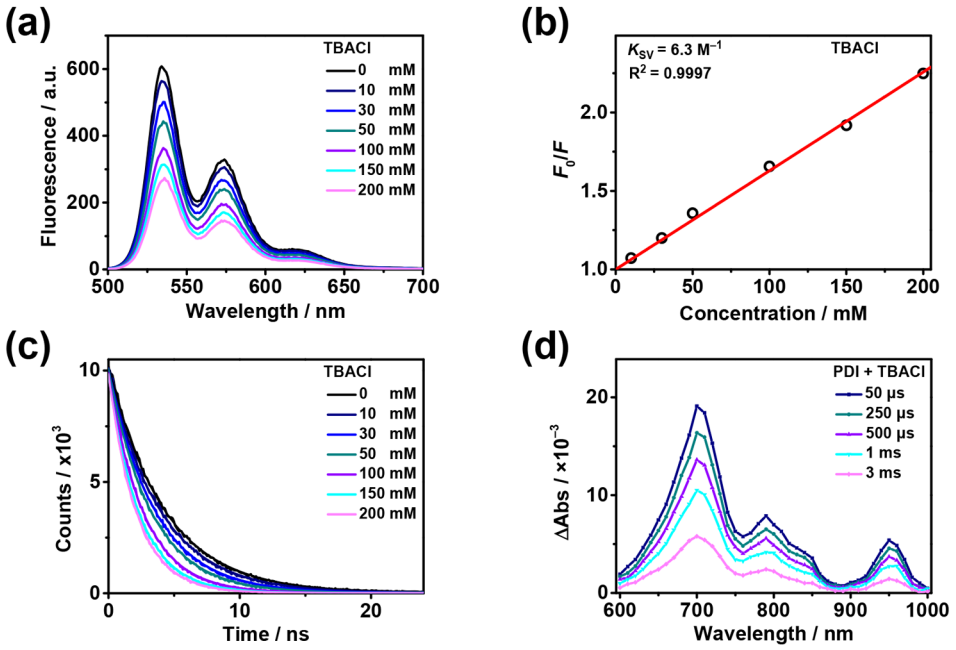

Figure 2. (a) Fluorescence spectra of PDI (λ_{ex} = 480 nm) upon titration of TBACl at indicated concentrations in CH_3CN solutions. (b) The corresponding Stern−Volmer plots for fluorescence intensity quenching. (c) Fluorescence lifetime decay of PDI (λ_{ex} = 450 nm) monitored at 535 nm upon titration of TBACl at indicated concentrations in CH_3CN solutions. (d) Transient absorption spectra of PDI in the presence of TBACl (200 mM) after 450 nm pulsed laser excitation at indicated time delays in CH_3CN solution under air.

$E^0(PDI/PDI^{\bullet-})$ = −0.26 V vs NHE. The addition of E_{0-0} to $E^0(PDI/PDI^{\bullet-})$ gave an approximation of the PDI excited state redox potential, $E^0(PDI^*/PDI^{\bullet-})$ = 2.09 V vs NHE.

To test if the PDI excited state is thermodynamically capable of lignin oxidation, CV was performed as well on these model compounds (Figure S1). The redox waves are irreversible, but the redox potentials for substrate oxidation could be approximated by the half-peak potential ($E_{p/2}$). The potentials span from 1.59−1.92 V and are well below $E^0(PDI^*/PDI^{\bullet-})$. The redox potential for the one-electron oxidation of chloride $E^0(Cl^{\bullet}/Cl^-)$ in CH_3CN is not well-defined. Past pulse radiolysis data suggested a potential of around 1.99 V in aqueous solution, while a recent study by the Meyer group estimated it to be approximately 1.45 V in CH_3CN. Caution is warranted due to possible significant deviations during error analysis.

Fluorescence quenching was carried out to interrogate the PDI excited state oxidizing power toward chloride oxidation. Figure 2a shows the fluorescence intensity changes of PDI in the presence of different concentrations of TBACl in a CH_3CN solution. As a comparison, the redox inert salt $TBAClO_4$ does not result in any fluorescence quenching (Figure S2).

https://doi.org/10.1021/acssuschemeng.3c04448
ACS Sustainable Chem. Eng. 2024, 12, 10−17

Table 1. Optimization Reaction Conditions of Visible-Light-Induced Cleavage of 1a[a]

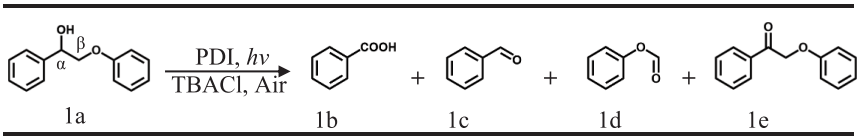

Entry	Deviation from standard conditions	Con. (%)	Yield of products (%)			
			1b	1c	1d	1e
1	Without TBACl	>99	54	9	20	n.d.
2	None	>99	70	21	74	2
3	$TBAClO_4$ instead of TBACl	>99	54	13	26	n.d.
4	TBABr instead of TBACl	53	2	5	n.d.	49
5	Ar instead of Air	25	n.d.	22	9	3
6	In the dark	n.r.	n.d.	n.d.	n.d.	n.d.
7	Without PDI	6	n.d.	3	n.d.	n.d.
8	TEMPO	9	n.d.	n.d.	n.d.	n.d.
9	10% TEOA	4	n.d.	n.d.	n.d.	n.d.
10	MeOH instead of CH_3CN	58	1	23	n.d.	2
11	Acetone instead of CH_3CN	>99	51	2	n.d.	n.d.

[a]Standard reaction conditions: 0.02 mmol substrate 1a, 20 mol % PDI, 40 mM TBACl, 2 mL CH_3CN, white light LED, air, 48 h, r.t. Yields of 1b, 1c, 1d, 1e = moles of product 1b, 1c, 1d, 1e formed/mol of substrate 1a input × 100%. n.r. = no reaction. n.d. = not detected. All yields were determined by HPLC analysis. TBABr, 40 mM; $TBAClO_4$, 40 mM; TEMPO, 40 mM.

Fluorescence lifetime measurements indicate that the PDI excited state quenching by TBACl is dynamic in nature (Figure 2c and Figure S3). No static component was observed, as solvation of ions in CH_3CN is efficient. Indeed, the ground-state absorption titration of PDI by TBACl did not show any measurable absorption peak shifts (Figure S4). The dynamic quenching constant (K_{SV}) obtained by the slope of the Stern–Volmer plot is around 6.3 M^{-1} (Figure 2b).

Fluorescence measurements did not reveal the underlying quenching mechanism, so nanosecond transient absorption spectroscopy was carried out to probe the photoinduced transient intermediates. Figure 2d shows the absorbance difference as a function of wavelength for PDI in the presence of TBACl after 450 nm of pulsed laser excitation. The spectra at variable delay times are all normalizable, indicating the formation of one transient state. The characteristic new absorption peaks at 700, 790, and 950 nm observed from the transient absorption spectra are consistent with the $PDI^{\bullet-}$ absorption (Figure S5), suggesting that the PDI excited state was reductively quenched by the chloride. Unfortunately, the oxidized species of chloride such as $Cl^{\bullet}$, Cl_2^-, or Cl_3^- only absorb appreciably in deep UV, preventing detection from the transient absorption spectra. Nevertheless, chloride is the only source of electrons. It is reasonable to infer a reductively quenching mechanism that involves the oxidation of chloride.

Fluorescence quenching was carried out as well for the lignin model substrates as the quenchers. The steady-state fluorescence intensity of PDI decreased upon titration of increasing concentrations of substrate 1a (Figure S6). UV–vis absorption spectra of PDI upon titration of substrate 1a did not show a ground-state association (Figure S7). Additionally, time-resolved fluorescence lifetime measurements demonstrated that PDI exhibited lifetime quenching in the presence of substrate 1a (Figure S8). Transient absorption spectra further indicated that the PDI excited state was reductively quenched by substrate 1a (Figure S9).

Thermodynamic and kinetic data indicate that the oxidation of the PDI excited state toward TBACl and substrate 1a is favorable. Next, to investigate both the selectivity and yield of the proposed light-induced Cl-atom-mediated C–C bond cleavage, 2-phenoxy-1-phenylethanol (substrate 1a) was chosen as the initial lignin model substrate (Table 1). The initial reactions in this study were carried out at room temperature and ambient conditions by irradiating the photocatalyst PDI with white light LED. Without TBACl, white light illumination resulted in oxidative cleavage of the lignin C–C bond with 99% conversion and satisfactory yields (54% for benzoic acid, 9% for benzaldehyde, and 20% for phenyl formate) (Table 1, entry 1). With the addition of TBACl, the yield of phenyl formate increased by 3.7-fold, and the overall yield of C–C cleavage products increased by 2-fold (Table 1, entry 2). The increased yield suggested chloride participation in the photocatalytic process where the Cl atom from chloride oxidation could act as a HAT reagent to activate C_β–H selectively and hence to cleave the C–C bond effectively. As a comparison, redox inert $TBAClO_4$ rather than TBACl had little influence on the yields of the four oxidized products (Table 1, entry 3). Then, replacing TBACl with TBABr only observed the undesired product 2-phenoxyacetophenone (1e) (Table 1, entry 4). This revealed that the oxidative power of Br atom ($E^0(Br^{\bullet}/Br^-)$ = 1.35 V vs NHE)[28] could only activate C_α–H, leading to the conversion of hydroxyl to ketone.

Running the reaction in Ar yielded only 22% benzaldehyde and 9% phenyl formate (Table 1, entry 5). This confirmed that O_2 was necessary as an electron acceptor for PDI regeneration. When the reaction was placed in the dark or without PDI, there was almost no conversion of substrate 1a, which indicated that light and the photocatalyst were both essential (Table 1, entries 6 and 7). Furthermore, substrate 1a was hardly converted after the addition of the radical trapping reagent 2,2,6,6-tetramethylpiperidine-1-oxyl (TEMPO) (Table 1, entry 8) or the sacrificial electron donor triethanolamine (TEOA) (Table 1, entry 9), indicating that the C–C bond was oxidatively cleaved and the reaction process involved radical intermediates. Compared with other solvents (Table 1, entries 10 and 11), CH_3CN was the preferred solvent to obtain effective and selective cleavage of the C–C bond.

https://doi.org/10.1021/acssuschemeng.3c04448
ACS Sustainable Chem. Eng. 2024, 12, 10–17

Table 2. Scope of Lignin Model Substrates under Visible-Light-Driven Cl-Atom-Mediated Oxidation[a]

Entry	Substrate	Con. (%)	Main Products (Yield, %)
2a	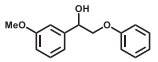	98	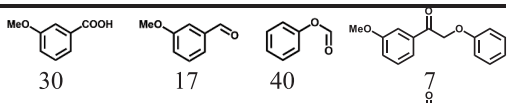 30 17 40 7
3a	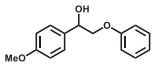	>99	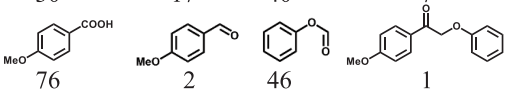 76 2 46 1
4a	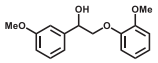	>99	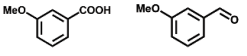 29 14
5a	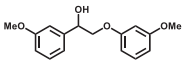	>99	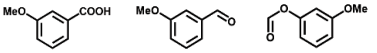 28 33 12
6a	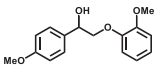	>99	 84 4
7a	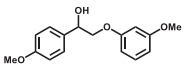	>99	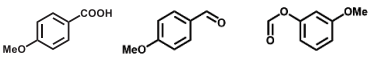 66 4 18
8a	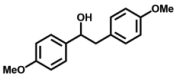	>99	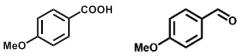 177 12
9a	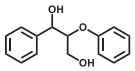	>99	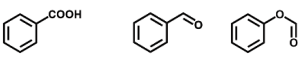 57 5 64
10a	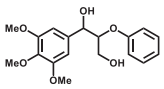	>99	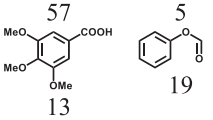 13 19
11a	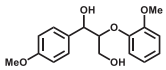	>99	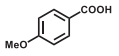 52
12a	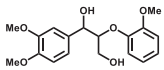	>99	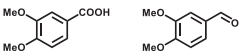 58 8
13a	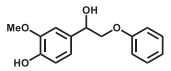	>99	 42
14a	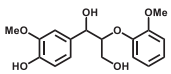	>99	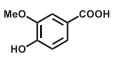 14

[a]Reaction conditions: 0.02 mmol substrate, 20 mol % PDI, 2 mL CH_3CN, visible light, air, 48 h, r.t. TBACl concentrations, 10a, 12a, 13a, 14a: 20 mM; 2a, 3a: 40 mM; 4a, 5a, 7a, 8a, 11a: 80 mM; 6a: 120 mM. 12a: 4 h. 14a: 3 h.

Furthermore, we also verified the applicability of photo-induced Cl atom-mediated C−C bond scission by other lignin models with different substitutions. It is well-known that the natural lignin structure contains a large number of methoxy-modified β−O−4 model skeletons. All substrates were almost completely converted within the range of model substrates (Table 2). The major cleavage products of single methoxy-substituted substrates 2a and 3a were the corresponding phenyl formate and methoxy-substituted benzoic acid (Table 2, entries 2a and 3a). The low cleavage yields of substrates 4a and 5a with two methoxy substituents may be caused by overoxidation of the substrates or intermediates (Table 2, entries 4a and 5a).[7] Substrates 6a and 7a with two methoxy substituents obtained *p*-methoxybenzoic acid as the main cleavage products (Table 2, entries 6a and 7a). In addition, a common β−1 bond backbone was also selected as the model substrate. The oxidative cleavage of the C−C bond in 1,2-diphenylethanol with methoxy-substitution resulted in 94.5% recovery of the aromatic compounds (Table 2, entry 8a). Substrates containing the C_γ−OH substituent, which makes the C−C bond more resistant to oxidation, also gave 99% conversion and 63% yield of aromatic compounds (Table 2, entry 9a). Model substrates with aliphatic primary alcohols and multiple methoxy substituents, which are prevalent in natural lignin linking units,[29−31] obtained a moderate yield of substituted aromatic acids (Table 2, entries 10a, 11a, and 12a). Moreover, photocatalytic experiments were also carried out on the model lignin compounds containing phenolic hydroxy groups (Table 2, entries 13a and 14a). The C−C bond of substrate 13a was also cleaved in moderate yields for phenyl formate. The substrate 14a led to a small amount of 3-methoxy-4-hydroxybenzoic acid in 3 h, but the product disappeared over an extended reaction time. The result may be the overoxidation of phenolic compounds to water-soluble

https://doi.org/10.1021/acssuschemeng.3c04448
ACS Sustainable Chem. Eng. 2024, 12, 10−17

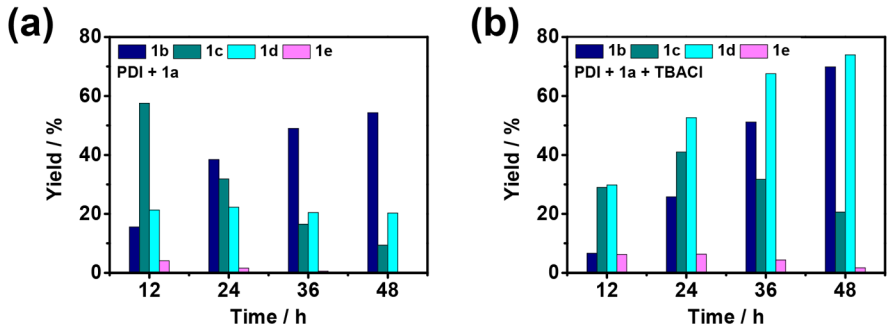

Figure 3. Product yields of photocatalytic 1a conversion in the absence of TBACl (a) and in the presence of TBACl (40 mM) (b) as a function of reaction time.

Scheme 1. Proposed Mechanism for C−C Bond Cleavage of Substrate 1a Induced by Visible-Light Excitation

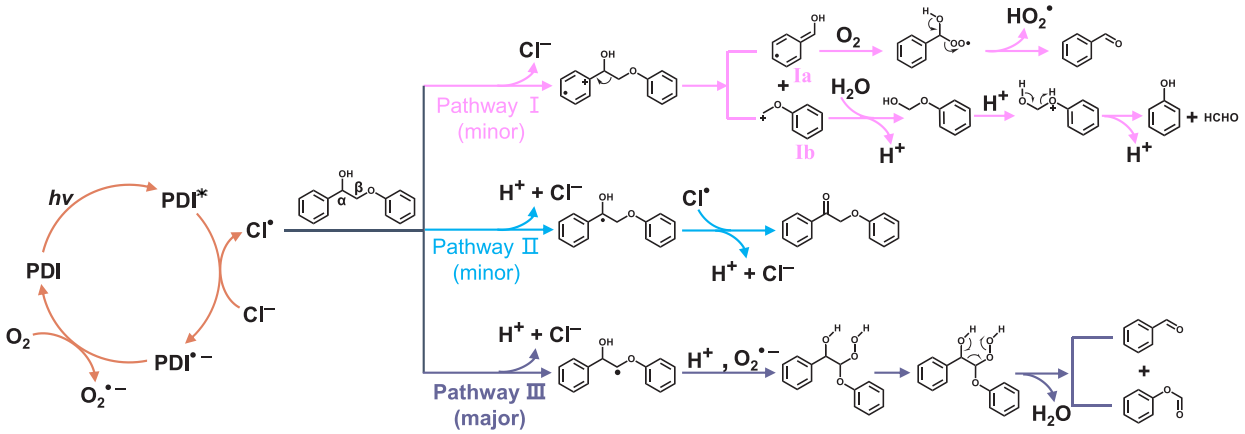

and/or polymeric species.[32] Note that no 2-methoxyphenyl formate was detected for 14a. This is likely due to the additional electron-donating methoxy substitution that lowers the redox potential for phenyl formate oxidation. Indeed, it was previously reported that 2-methoxyphenyl formate hydrolyzed to guaiacol[6] that was unstable under photocatalytic oxidation conditions.[33] Guaiacol was then subject to further over-oxidation or polymerization.[7] Taken together, it is reasonable that no 2-methoxyphenyl formate was obtained after cleavage of the substrate of entry 14a.

In addition, we also monitored the product yields of C−C bond cleavage for all substrates in the presence of different concentrations of TBACl (Table S2). Combined with the analysis of the oxidation potential of these substrates, the Cl atom mediated efficient and selective cleavage of the model substrate C−C bond in an ambient environment. Encouraged by these results, we further investigated the feasibility of Cl-atom-mediated cleavage of natural lignin sources of pine extracts. Several depolymerized aromatic components in the crude reaction mixture were confirmed by GC-MS (Figure S10). The main products are aromatic aldehydes and monophenolic compounds. Some of the products are high value chemicals, such as vanillin, syringaldehyde, and so on. The preliminary results show that this photocatalytic strategy can effectively realize real lignin valorization by using sunlight.

To accurately illustrate the evolution of the reaction intermediate, we further monitored the product yield of C−C bond cleavage as a function of reaction time. As shown in Figure 3a, with prolonged reaction time, the yield of benzoic acid gradually increased while benzaldehyde decreased, and phenyl formate hardly changed. However, in the presence of TBACl (Figure 3b), the yield of phenyl formate gradually increased, and a satisfactory cleavage yield could be achieved. Combined with the analysis of control experiments (Table S3), benzoic acid was derived from the deep oxidation of benzaldehyde by oxygen as the terminal oxidant. Although part of the unwanted 2-phenoxyacetophenone product was formed during the reaction, the strong oxidative power of the excited state of PDI eventually cleaved it to benzoic acid and phenyl formate without any additional sacrificial agent. Control experiments showed that the final aromatic products benzoic acid and phenyl formate existed stably in the reaction system.

TA experiments confirmed that the PDI excited state acts as a sufficiently powerful oxidant to oxidize the substrate and Cl^- through electron transfer rather than energy transfer. This process also results in the simultaneous generation of a PDI radical anion ($PDI^{\bullet-}$). The fluorescence titration experiment also clarified that Cl^- can quench the excited state of the photocatalyst PDI in the presence of 1a (Figure S11). In particular, radical trapping experiments in the presence of 1,1-diphenylethylene further illustrated that Cl atoms can be obtained by PDI excited state single-electron oxidation (Figure S12). Combined with the cleavage products and percent yields of the model substrates in Tables 1 and 2, the possible mechanism of photocatalytic C−C bond cleavage is proposed in Scheme 1.

First, single-electron oxidation of Cl^- by excited state PDI produces a Cl atom accompanied by the appearance of $PDI^{\bullet-}$ under visible-light irradiation. $PDI^{\bullet-}$ is allowed to transfer to the electron acceptor O_2 to form a superoxide anion ($O_2^{\bullet-}$) (Figure S13), thereby regenerating the photocatalyst PDI. Subsequently, the highly reactive Cl atom has the potential to

https://doi.org/10.1021/acssuschemeng.3c04448
ACS Sustainable Chem. Eng. 2024, 12, 10−17

cleave the C−C bond from the following three different possible pathways. Pathway I is similar to the enzyme-promoted C−C bond fragmentation reactions of lignin model compounds by single-electron transfer.[34−37] The initial step of pathway I is the oxidation of the electron-rich benzene ring of substrate 1a to form a radical (arene) cation.[36,38,39] The C−C bond heterolytic cleavage of the radical cation intermediate produces a radical cation pair in which the radical resides on the fragment Ia and the positive charge on the aryloxyalkyl Ib.[40] The radical fragment Ia reacts with O_2 to form the peroxyl radical, which further decomposes to produce benzaldehyde.[40,41] The positively charged aryloxyalkyl Ib reacts with H_2O to form phenol.[40,42] However, no such phenolic products were observed in Tables 1 and 2. It is possible that the phenolic compounds were overoxidized to water-soluble and/or polymeric species under the reaction conditions and therefore were not detected.[32,41,43] Furthermore, we note that in the cleavage products in Tables 1 (entry 2) and 2 (entries 2a, 3a, 5a, and 7a), the yields of aromatic aldehydes and acids are always greater than the yields of phenyl formate (with or without methoxy substitution), and the molar ratio is not close to 1:1. A possible explanation is that pathway I is a minor reaction route to produce phenolic components that are further overoxidized to water-soluble and/or polymeric species. Pathway II suggests that the Cl atom extracts the C_α−H proton from substrate 1a to form oxidized ketone intermediates with further cleavage of the C−C bond. However, we note that the cleavage of 1a produces a large amount of benzaldehyde (Figure 3b), whereas the oxidized ketone 1e cleaves directly to benzoic acid without benzaldehyde (Figure S14), so this pathway is also a minor cleavage route. With Pathways I and II being the minor routes, Pathway III is thereby the major reaction route to the final products. The highly reactive Cl atom is responsible for the selective abstraction of hydrogen atoms in model substrate 1a C_β−H to generate C_β-centered radical and release protons. Next, the C_β-centered radical reacts with $O_2^{\bullet-}$ and the released proton to form an unstable peroxide intermediate, which, in turn, induces C−C bond cleavage to form benzaldehyde and water. Control experiments show that benzaldehyde is further oxidized to benzoic acid.

In summary, we have successfully developed a new strategy for the visible-light-mediated C−C bond cleavage of lignin model substrates in an additive-free and metal-free manner under ambient conditions. By combining PDI photoredox catalysis and TBACl as a Cl atom source, we have achieved efficient and selective cleavage of the C−C bond in β−O−4 linkages model substrates, with 99% conversion and 82.5% recovery of the monomeric aromatics. Moreover, the cleavage of the β−1 linkage model substrate also achieved high selectivity and yields with the assistance of Cl atom intermediate as the HAT catalyst. This photocatalytic strategy, which exploits Cl atom to promote C−C bond cleavage with a cheap and inexpensive organicphotocatalyst, PDI, opens up new avenues for lignin valorization.

■ ASSOCIATED CONTENT

Supporting Information

The Supporting Information is available free of charge at https://pubs.acs.org/doi/10.1021/acssuschemeng.3c04448.

Experimental details, additional electrochemical and spectroscopic characterizations, and GC-MS analysis for Cl atom trapping species (PDF)

■ AUTHOR INFORMATION

Corresponding Author

Ke Hu − *Department of Chemistry and Shanghai Key Laboratory of Molecular Catalysis and Innovative Materials, Fudan University, Shanghai 200433, P. R. China;* orcid.org/0000-0002-0240-7192; Email: khu@fudan.edu.cn

Authors

Pengju Li − *Department of Chemistry and Shanghai Key Laboratory of Molecular Catalysis and Innovative Materials, Fudan University, Shanghai 200433, P. R. China*

Rong Liu − *Department of Chemistry and Shanghai Key Laboratory of Molecular Catalysis and Innovative Materials, Fudan University, Shanghai 200433, P. R. China*

Zijian Zhao − *Department of Chemistry and Shanghai Key Laboratory of Molecular Catalysis and Innovative Materials, Fudan University, Shanghai 200433, P. R. China*

Weijian Yang − *Department of Chemistry and Shanghai Key Laboratory of Molecular Catalysis and Innovative Materials, Fudan University, Shanghai 200433, P. R. China*

Fushuang Niu − *Department of Chemistry and Shanghai Key Laboratory of Molecular Catalysis and Innovative Materials, Fudan University, Shanghai 200433, P. R. China*

Limei Tian − *Department of Chemistry and Shanghai Key Laboratory of Molecular Catalysis and Innovative Materials, Fudan University, Shanghai 200433, P. R. China*

Complete contact information is available at: https://pubs.acs.org/10.1021/acssuschemeng.3c04448

Notes

The authors declare no competing financial interest.

■ ACKNOWLEDGMENTS

This work is supported by the National Natural Science Foundation of China (22173022) and Natural Science Foundation of Shanghai (21ZR1404400, 19DZ2270100).

■ REFERENCES

(1) Cui, T.; Ma, L.; Wang, S.; Ye, C.; Liang, X.; Zhang, Z.; Meng, G.; Zheng, L.; Hu, H.-S.; Zhang, J.; Duan, H.; Wang, D.; Li, Y. Atomically dispersed Pt−N3C1 sites enabling efficient and selective electrocatalytic C−C bond cleavage in lignin models under ambient conditions. *J. Am. Chem. Soc.* **2021**, *143*, 9429−9439.

(2) Li, S.; Kim, S.; Davis, A. H.; Zhuang, J.; Shuler, E. W.; Willinger, D.; Lee, J.-J.; Zheng, W.; Sherman, B. D.; Yoo, C. G.; Leem, G. Photocatalytic chemoselective C−C bond cleavage at room temperature in dye-sensitized photoelectrochemical cells. *ACS Catal.* **2021**, *11*, 3771−3781.

(3) Liu, H.; Li, H.; Luo, N.; Wang, F. Visible-light-induced oxidative lignin C−C bond cleavage to aldehydes using vanadium catalysts. *ACS Catal.* **2020**, *10*, 632−643.

(4) Hu, Y.; Yan, L.; Zhao, X.; Wang, C.; Li, S.; Zhang, X.; Ma, L.; Zhang, Q. Mild selective oxidative cleavage of lignin C−C bonds over a copper catalyst in water. *Green Chem.* **2021**, *23*, 7030−7040.

(5) Zhu, G.; Shi, S.; Zhao, L.; Liu, M.; Gao, J.; Xu, J. Catalytic activation of carbon−hydrogen bonds in lignin linkages over strong-base-modified covalent triazine frameworks for lignin oxidative cleavage. *ACS Catal.* **2020**, *10*, 7526−7534.

(6) Gazi, S.; Đokić, M.; Moeljadi, A. M. P.; Ganguly, R.; Hirao, H.; Soo, H. S. Kinetics and DFT studies of photoredox carbon−carbon bond cleavage reactions by molecular vanadium catalysts under ambient conditions. *ACS Catal.* **2017**, *7*, 4682−4691.
(7) Liu, H.; Li, H.; Lu, J.; Zeng, S.; Wang, M.; Luo, N.; Xu, S.; Wang, F. Photocatalytic cleavage of C−C bond in lignin models under visible light on mesoporous graphitic carbon nitride through $\pi-\pi$ stacking interaction. *ACS Catal.* **2018**, *8*, 4761−4771.
(8) Hou, T.; Luo, N.; Li, H.; Heggen, M.; Lu, J.; Wang, Y.; Wang, F. Yin and yang dual characters of CuOx clusters for C−C bond oxidation driven by visible light. *ACS Catal.* **2017**, *7*, 3850−3859.
(9) Bosque, I.; Magallanes, G.; Rigoulet, M.; Kärkäs, M. D.; Stephenson, C. R. J. Redox catalysis facilitates lignin depolymerization. *ACS Cent. Sci.* **2017**, *3*, 621−628.
(10) Liu, M.; Zhang, Z.; Song, J.; Liu, S.; Liu, H.; Han, B. Nitrogen dioxide catalyzed aerobic oxidative cleavage of C (OH)−C bonds of secondary alcohols to produce acids. *Angew. Chem., Int. Ed.* **2019**, *131*, 17554−17559.
(11) Ota, E.; Wang, H.; Frye, N. L.; Knowles, R. R. A redox strategy for light-driven, out-of-equilibrium isomerizations and application to catalytic C−C bond cleavage reactions. *J. Am. Chem. Soc.* **2019**, *141*, 1457−1462.
(12) Nguyen, S. T.; Murray, P. R. D.; Knowles, R. R. Light-driven depolymerization of native lignin enabled by proton-coupled electron transfer. *ACS Catal.* **2020**, *10*, 800−805.
(13) Wang, Y.; Liu, Y.; He, J.; Zhang, Y. Redox-neutral photocatalytic strategy for selective C−C bond cleavage of lignin and lignin models via PCET process. *Sci. Bull.* **2019**, *64*, 1658−1666.
(14) Nutting, J. E.; Rafiee, M.; Stahl, S. S. Tetramethylpiperidine N-Oxyl (TEMPO), phthalimide N-Oxyl (PINO), and related N-Oxyl species: electrochemical properties and their use in electrocatalytic reactions. *Chem. Rev.* **2018**, *118*, 4834−4885.
(15) Beejapur, H. A.; Zhang, Q.; Hu, K.; Zhu, L.; Wang, J.; Ye, Z. TEMPO in chemical transformations: from homogeneous to heterogeneous. *ACS Catal.* **2019**, *9*, 2777−2830.
(16) Rafiee, M.; Alherech, M.; Karlen, S. D.; Stahl, S. S. Electrochemical aminoxyl-mediated oxidation of primary alcohols in lignin to carboxylic acids: polymer modification and depolymerization. *J. Am. Chem. Soc.* **2019**, *141*, 15266−15276.
(17) Rohe, S.; Morris, A. O.; McCallum, T.; Barriault, L. Hydrogen atom transfer reactions via photoredox catalyzed chlorine atom generation. *Angew. Chem., Int. Ed.* **2018**, *57*, 15664−15669.
(18) Deng, H. P.; Zhou, Q.; Wu, J. Microtubing-reactor-assisted aliphatic C−H functionalization with HCl as a hydrogen-atom-transfer catalyst precursor in conjunction with an organic photoredox catalyst. *Angew. Chem., Int. Ed.* **2018**, *130*, 12843−12847.
(19) Treacy, S. M.; Rovis, T. Copper catalyzed C(sp3)−H bond alkylation via photoinduced ligand-to-metal charge transfer. *J. Am. Chem. Soc.* **2021**, *143*, 2729−2735.
(20) Jia, P.; Li, Q.; Poh, W. C.; Jiang, H.; Liu, H.; Deng, H.; Wu, J. Light-promoted bromine-radical-mediated selective alkylation and amination of unactivated C (sp3)−H bonds. *Chem.* **2020**, *6*, 1766−1776.
(21) Li, Z.; Luo, L.; Li, M.; Chen, W.; Liu, Y.; Yang, J.; Xu, S.-M.; Zhou, H.; Ma, L.; Xu, M.; Kong, X.; Duan, H. Photoelectrocatalytic C−H halogenation over an oxygen vacancy-rich TiO2 photoanode. *Nat. Commun.* **2021**, *12*, 1−13.
(22) Yuan, R.; Fan, S.; Zhou, H.; Ding, Z.; Lin, S.; Li, Z.; Zhang, Z.; Xu, C.; Wu, L.; Wang, X.; Fu, X. Chlorine-radical-mediated photocatalytic activation of C-H bonds with visible light. *Angew. Chem., Int. Ed.* **2013**, *125*, 1069−1073.
(23) Li, P.; Deetz, A. M.; Hu, J.; Meyer, G. J.; Hu, K. Chloride oxidation by one-or two-photon excitation of N-Phenylphenothiazine. *J. Am. Chem. Soc.* **2022**, *144*, 17604−17610.
(24) Ohkubo, K.; Fujimoto, A.; Fukuzumi, S. Metal-free oxygenation of cyclohexane with oxygen catalyzed by 9-mesityl-10-methylacridinium and hydrogen chloride under visible light irradiation. *Chem. Commun.* **2011**, *47*, 8515−8517.
(25) Deetz, A. M.; Troian-Gautier, L.; Wehlin, S. A.; Piechota, E. J.; Meyer, G. J. On the determination of halogen atom reduction potentials with photoredox catalysts. *J. Phys. Chem. A* **2021**, *125*, 9355−9367.
(26) Troian-Gautier, L.; Turlington, M. D.; Wehlin, S. A.; Maurer, A. B.; Brady, M. D.; Swords, W. B.; Meyer, G. J. Halide photoredox chemistry. *Chem. Rev.* **2019**, *119*, 4628−4683.
(27) Ghosh, I.; Ghosh, T.; Bardagi, J. I.; König, B. Reduction of aryl halides by consecutive visible light-induced electron transfer processes. *Science* **2014**, *346*, 725−728.
(28) Bevernaegie, R.; Wehlin, S. A. M.; Piechota, E. J.; Abraham, M.; Philouze, C.; Meyer, G. J.; Elias, B.; Troian-Gautier, L. Improved visible light absorption of potent Iridium(III) photo-oxidants for excited-State electron transfer chemistry. *J. Am. Chem. Soc.* **2020**, *142*, 2732−2737.
(29) Nguyen, S. T.; Murray, P. R.; Knowles, R. R. Light-driven depolymerization of native lignin enabled by proton-coupled electron transfer. *ACS Catal.* **2020**, *10*, 800−805.
(30) Cui, T.; Ma, L.; Wang, S.; Ye, C.; Liang, X.; Zhang, Z.; Meng, G.; Zheng, L.; Hu, H.-S.; Zhang, J.; Duan, H.; Wang, D.; Li, Y. Atomically dispersed Pt−N3C1 sites enabling efficient and selective electrocatalytic C−C bond cleavage in lignin models under ambient conditions. *J. Am. Chem. Soc.* **2021**, *143*, 9429−9439.
(31) Bosque, I.; Magallanes, G.; Rigoulet, M.; Kärkäs, M. D.; Stephenson, C. R. Redox catalysis facilitates lignin depolymerization. *ACS Cent. Sci.* **2017**, *3*, 621−628.
(32) Baciocchi, E.; Fabbri, C.; Lanzalunga, O. Lignin peroxidase-catalyzed oxidation of nonphenolic trimeric lignin model compounds: fragmentation reactions in the intermediate radical cations. *J. Org. Chem.* **2003**, *68*, 9061−9069.
(33) Cao, Y.-X.; Zhu, G.; Li, Y.; Le Breton, N.; Gourlaouen, C.; Choua, S.; Boixel, J.; Jacquot de Rouville, H.-P.; Soulé, J.-F. Photoinduced arylation of acridinium salts: tunable photoredox catalysts for C−O bond cleavage. *J. Am. Chem. Soc.* **2022**, *144*, 5902−5909.
(34) Zhou, W.; Nakahashi, J.; Miura, T.; Murakami, M. Light/copper relay for aerobic fragmentation of lignin model compounds. *Asian J. Org. Chem.* **2018**, *7*, 2431−2434.
(35) Cho, D. W.; Latham, J. A.; Park, H. J.; Yoon, U. C.; Langan, P.; Dunaway-Mariano, D.; Mariano, P. S. Regioselectivity of enzymatic and photochemical single electron transfer promoted carbon− carbon bond fragmentation reactions of tetrameric lignin model compounds. *J. Org. Chem.* **2011**, *76*, 2840−2852.
(36) Miki, K.; Renganathan, V.; Gold, M. H. Mechanism of. beta.-aryl ether dimeric lignin model compound oxidation by lignin peroxidase by Phanerochaete chrysosporium. *Biochemistry* **1986**, *25*, 4790−4796.
(37) Umezawa, T.; Higuchi, T. Mechanism of aromatic ring cleavage of β-O-4 lignin substructure models by lignin peroxidase. *FEBS Lett.* **1987**, *218*, 255−260.
(38) Cho, D. W.; Parthasarathi, R.; Pimentel, A. S.; Maestas, G. D.; Park, H. J.; Yoon, U. C.; Dunaway-Mariano, D.; Gnanakaran, S.; Langan, P.; Mariano, P. S. Nature and kinetic analysis of carbon−carbon bond fragmentation reactions of cation radicals derived from set-oxidation of lignin model compounds. *J. Org. Chem.* **2010**, *75*, 6549−6562.
(39) Wu, X.; Lin, J.; Zhang, H.; Xie, S.; Zhang, Q.; Sels, B. F.; Wang, Y. Z-Scheme nanocomposite with high redox ability for efficient cleavage of lignin C−C bonds under simulated solar light. *Green Chem.* **2021**, *23*, 10071−10078.
(40) Ten Have, R.; Teunissen, P. J. Oxidative mechanisms involved in lignin degradation by white-rot fungi. *Chem. Rev.* **2001**, *101*, 3397−3414.
(41) Tien, M.; Kirk, T. K. Lignin-degrading enzyme from Phanerochaete chrysosporium: purification, characterization, and catalytic properties of a unique H2O2-requiring oxygenase. *Proc. Natl. Acad. Sci. U. S. A.* **1984**, *81*, 2280−2284.

https://doi.org/10.1021/acssuschemeng.3c04448
ACS Sustainable Chem. Eng. 2024, 12, 10−17

(42) Hammel, K. E.; Jensen, K. A., Jr; Mozuch, M. D.; Landucci, L. L.; Tien, M.; Pease, E. A. Ligninolysis by a purified lignin peroxidase. *J. Biol. Chem.* **1993**, *268*, 12274−12281.
(43) Kirk, T. K.; Tien, M.; Kersten, P. J.; Mozuch, M. D.; Kalyanaraman, B. Ligninase of phanerochaete chrysosporium. Mechanism of its degradation of the non-phenolic arylglycerol *β*-aryl ether substructure of lignin. *Biochem. J.* **1986**, *236*, 279−287.

https://doi.org/10.1021/acssuschemeng.3c04448
ACS Sustainable Chem. Eng. 2024, 12, 10−17